ELSEVIER

Catalysis Today 82 (2003) 141–150

CATALYSIS TODAY

www.elsevier.com/locate/cattod

Dense ceramic membranes for methane conversion

Henny J.M. Bouwmeester

Laboratory for Inorganic Materials Science, Department of Science and Technology & MESA+ Research Institute, University of Twente, 7500 AE Enschede, The Netherlands

Abstract

Dense ceramic membranes made from mixed oxygen-ionic and electronic conducting perovskite-related oxides allow separation of oxygen from an air supply at elevated temperatures (>700 °C). By combining air separation and catalytic partial oxidation of methane to syngas into a ceramic membrane reactor, this technology is expected to significantly reduce the capital costs of conversion of natural gas to liquid added-value products. The present survey is mainly concerned with the material properties that govern the performance of the mixed-conducting membranes in real operating conditions and highlights significant developments in the field.
© 2003 Elsevier B.V. All rights reserved.

Keywords: Dense ceramic membranes; Methane conversion; Perovskite

1. Introduction

Ceramic membranes made from mixed oxygen-ionic and electronic conducting (MIEC) perovskite oxides can selectively separate oxygen from air at elevated temperatures, typically higher than 700 °C [1]. These membranes are promising for use in many industrial processes that require a continuous supply of pure oxygen. Over the past several years, extensive efforts have focused on using the MIEC membranes to improve the performance of methane conversion processes, i.e. combining air separation and high-temperature catalytic partial oxidation (CPO) into a single step. Of particular significance is the partial oxidation of methane to syngas ($CO + H_2$). Excellent methane conversion levels have been reported and CO selectivities are found to approach 100% in the presence of a reliable catalyst, e.g. supported Ni or Rh. The H_2:CO ratio of 2:1 of the syngas produced by CPO makes it an ideal feedstock for the gas-to-liquid production of natural gas to liquid fuels via existing processes, such as Fisher–Tropsch and methanol synthesis [2–6]. Successful development of the MIEC membrane reactor technology eliminates the need for expensive oxygen produced by cryogenic means. The technology is compact and modular, and thus allows access to remote sources of natural gas. An external energy supply is not needed due to the exothermicity of the CPO reaction. The ceramic membrane further aids in safety management, since it avoids the premixing of oxygen and natural gas and reduces the formation of hot spots as encountered in a co-feed reactor. In addition, the technology can be used for the production of hydrogen, particularly for the set up of distributed hydrogen production capacities. Recognising the potential advantages and economic benefits offered by this technology relative to conventional steam reforming or partial oxidation, world-wide alliances co-ordinated by Air Products and Praxair, respectively, have been founded to solve the scale-up problems. For syngas production, the

E-mail address: h.j.mbouwmeester@utwente.nl (H.J.M. Bouwmeester).

0920-5861/$ – see front matter © 2003 Elsevier B.V. All rights reserved.
doi:10.1016/S0920-5861(03)00222-0

ceramic membrane must be able to tolerate long-term exposure to severe chemical potential gradients, with air on one side and natural gas on the other side of the membrane. Successful implementation demands that membrane materials must be identified with a required performance in terms of oxygen flux, chemical stability and mechanical reliability [6].

This paper first briefly discusses some of the fundamentals of MIEC perovskite membranes and issues related to membrane stability. It then highlights some recent developments of their use in catalytic membrane reactors for methane conversion processes.

2. Principle of operation

The operating principle of an MIEC membrane is illustrated in Fig. 1. By imposing an oxygen partial pressure differential across the membrane oxygen is driven from the high partial pressure side to the low partial pressure side. In a typical membrane reactor, the pressure differential is provided by air on one side and a reducing gas, i.e. depleting the oxygen partial pressure by a chemical reaction, on the other side of the membrane. The ceramic membrane facilitates separation of oxygen from the air supply with infinite selectivity, provided that it is fabricated dense, i.e. free of cracks and connected-through porosity. Owing to the ability to conduct both oxygen ions and electronic charge carriers, it operates without the need of electrodes and external circuitry, in contrast with solid oxide fuel cells and oxygen pumps. The presence of

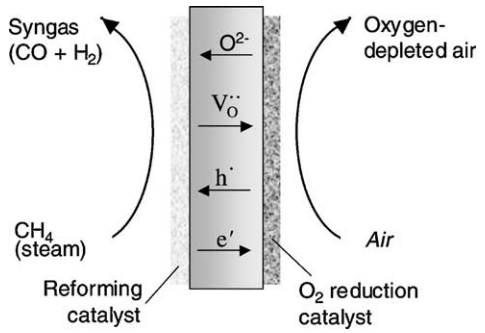

Fig. 1. Operating principle of a ceramic membrane reactor for the partial oxidation of methane to syngas.

electronic conductivity in the MIEC thereby acts as an internal short-circuit for electrons (or holes) to counteract the flux of oxygen anions.

Much of the research efforts in this field are focused on acceptor-doped perovskite oxides $La_{1-x}A_xCo_{1-y}B_yO_{3-\delta}$ (A = Sr, Ba; B = Fe, Cr, Mn, Ga). Compositions like these were first explored by Teraoka et al. [7,8]. The partial substitution of metal cations in the ABO_3 perovskite structure by cations with lower valencies leads to the formation of oxygen vacancies. Vacancies also arise due to equilibration of the perovskite oxide at reduced oxygen partial pressure. Disordering of the oxygen vacancies at elevated temperatures leads to the onset of ionic conductivity. For example, in the series $La_{1-x}Sr_xCo_{1-y}Fe_yO_{3-\delta}$, the ionic conductivity, in air, at temperatures 700–1000 °C can be one to two orders of magnitude larger than that of known zirconia-based solid electrolytes [9]. The presence of multivalent cations in the perovskite compositions ensures a high, often predominating electronic conductivity.

Electronic conduction in oxygen-ion conducting fluorite-type ceramics can be enhanced by dissolution of oxides having multivalent cations. A notable example is yttria-stabilised zirconia (YSZ) doped with multivalent cations, such as Ce, Pr, Ti, and Tb. The extent of mixed conductivity in fluorite-oxide ceramics is often orders of magnitude less than those found for selected acceptor-doped perovskite-type oxides. Alternatively, the internal short-circuit function is obtained by dispersion of an electronic conducting phase, usually a noble metal, in the oxygen ion conducting ceramics, for example, YSZ–Pt. The concentrations of constituent phases must be high enough to provide percolative pathways for both ionic and electronic charge carriers across the membrane. Neither membranes made from doped fluorite-type ceramics nor dual-phase composite membranes are considered any further in this review. For a survey on ceramic oxygen ion conducting membranes, see Ref. [1].

3. Theory of oxygen transport through perovskite membranes

Classical Wagner theory is usually adopted to express the flux of oxygen through MIEC membranes

exposed to an oxygen chemical potential gradient [10]:

$$j_{O_2} = -\frac{1}{4^2F^2}\frac{\sigma_{ion}\sigma_{el}}{\sigma_{ion}+\sigma_{el}}\nabla\mu_{O_2} \quad (1)$$

where σ_{ion} and σ_{el} are the partial conductivities provided by oxygen ionic and electronic defects, respectively; $\nabla\mu_{O_2}$ the gradient in oxygen chemical potential and other parameters have their usual significance. Eq. (1) is valid provided that the surface reactions at both sides of the membrane are fast enough and do not exert any influence on overall oxygen transport. Assuming predominant electronic conductivity, Eq. (1) can be simplified to

$$j_{O_2} = -\frac{\sigma_{ion}}{4^2F^2}\nabla\mu_{O_2} \quad (2)$$

This equation may be recast through the use of the Nernst–Einstein equation in a form that includes the individual diffusion coefficient for oxygen vacancies:

$$j_{O_2} = -\frac{c_V D_V}{4RT}\nabla\mu_{O_2} \quad (3)$$

where D_V is the vacancy diffusion coefficient and c_V the concentration of mobile oxygen vacancies. Assuming that all oxygen vacancies are free and contribute to ionic transport, and that the value of D_V is approximately constant over the experimental range in oxygen nonstoichiometry, integration of Eq. (3) over membrane thickness L yields:

$$j_{O_2} \approx -\frac{D_V}{4L}\int_{\ln p''_{O_2}}^{\ln p'_{O_2}} c_V \ln p_{O_2} \quad (4)$$

The limits of integration are the oxygen partial pressures maintained at opposite sides of the membrane. Data of oxygen nonstoichiometry for a simple perovskite like $La_{0.9}Sr_{0.1}FeO_{3-\delta}$ obtained from thermogravimetry data by Mizusaki et al. [11] are shown in Fig. 2. Eq. (4) predicts that the magnitude of the oxygen flux is proportional to the dashed area in Fig. 2. The ability of Eq. (4) to quantitatively fit experimental data of oxygen permeation is illustrated for $La_{1-x}Sr_xFeO_{3-\delta}$ ($x = 0.1$–0.4) in Fig. 3a [12]. The value of D_V thus obtained for $La_{0.9}Sr_{0.1}FeO_{3-\delta}$ shows reasonable agreement with the corresponding value obtained from oxygen isotopic exchange as shown in Fig. 3b. Higher oxygen fluxes would thus be facilitated if the $ABO_{3-\delta}$ perovskite composition exhibits larger concentrations of oxygen vacancies, i.e. with increased A-site substitution and a higher reducibility of the transition metal ions occupying the B-site. Note from Fig. 2 that the oxygen partial pressure maintained at the oxygen-lean side of the membrane has a most significant influence on the oxygen flux.

Using the above equations it is possible to construct the oxygen chemical potential profile across the MIEC membrane at steady state. Evaluation can be carried out by integration of Eq. (3) up to depth x into the membrane, which integral equals the

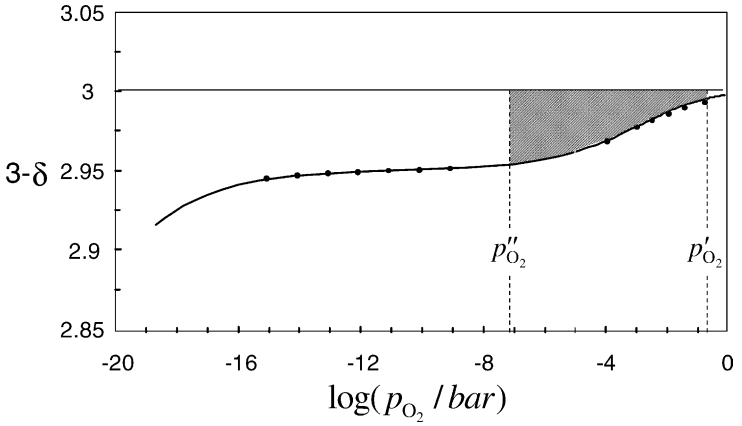

Fig. 2. Oxygen nonstoichiometry data for $La_{0.9}Sr_{0.1}FeO_{3-\delta}$ at 1000 °C. The solid line is from a random point defect model (reproduced from Mizusaki et al. [11]). If all oxygen vacancies contribute to ionic transport, the oxygen flux is proportional to the shaded area. p'_{O_2} and p''_{O_2} are the oxygen partial pressures at opposite sides of the membrane.

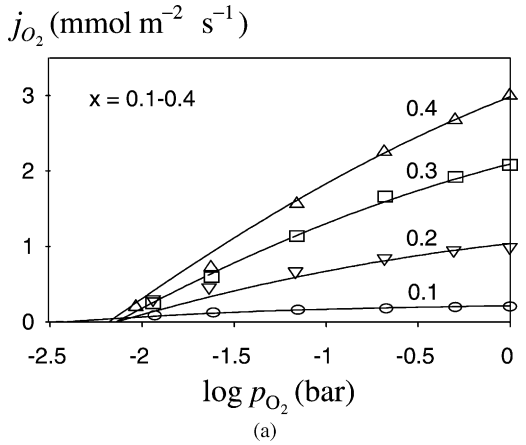

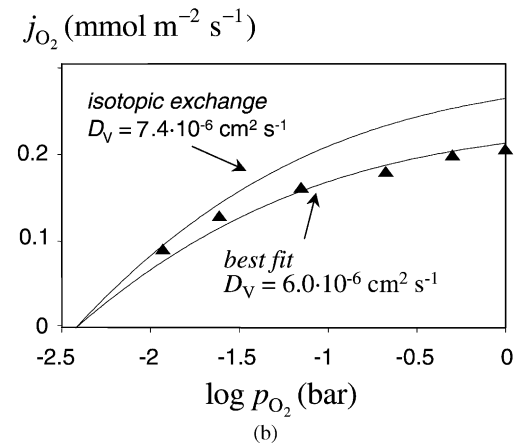

Fig. 3. (a) Theoretical modelling of feed-side p_{O_2}-dependence of oxygen permeation through $La_{1-x}Sr_xFeO_{3-\delta}$ ($x = 0.1$–0.4) at 1000 °C. (b) The best fit for $La_{0.9}Sr_{0.1}FeO_{3-\delta}$ is obtained when D_V equals 6×10^{-6} cm^2 s^{-1}, which deviates slightly from the corresponding value obtained from data of isotopic exchange (reproduced from ten Elshof et al. [12]).

result of Eq. (4). (Provided that D_V can be treated as a constant, it is required from Eq. (3) that the product $c_V \cdot \nabla\mu_{O_2}$ is constant throughout the membrane.) Fig. 4 schematically depicts the oxygen chemical potential profile across the MIEC membrane, taking into account possible losses in the driving force for oxygen transport associated with a limited rate of the surface reactions. Enhancing the membrane surface area and/or coating an appropriate catalyst directly on the membrane surface can minimise the interfacial losses.

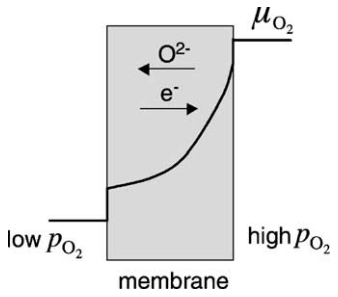

Fig. 4. Schematic illustration of the profile in oxygen chemical potential μ_{O_2} across the MIEC membrane at steady-state conditions.

4. Vacancy ordering

For complex oxide systems, the onset of defect interactions and propensity to form ordered structures progressively grow with increasing defect concentrations. Defect association and ordering of oxygen vacancies can induce significant changes in the ionic conductivity, as is known for oxides that crystallise in the fluorite structure, such as CeO_2, ThO_2 and ZrO_2. These oxides can accommodate a large fraction of lower-valent cations, such as calcium and yttrium, which is charge compensated by the formation of oxygen vacancies. In many cases, a maximum is observed in the conductivity at doping levels which correspond to 5–8% oxygen vacancies [13]. In the acceptor-doped perovskite oxides, it is not uncommon to have an oxygen deficiency of 10–15% or more. Superlattice ordering rather than defect association is more favoured, which results from the very effective screening of defect charges in the perovskite-related oxides that are highly polarisible [14].

The well-known brownmillerite structure with ideal stoichiometry $A_2B_2O_5$ can be derived from the cubic ABO_3 perovskite lattice by regularly removing one-sixth of the oxygen atoms. The oxygen deficiency is thus 16.7%. As is shown in Fig. 4, the ordering of oxygen vacancies in the [1 0 1] direction creates layers of corner-shared BO_6 octahedra, alternating with corner-shared BO_4 tetrahedra. As a matter of fact, vacancy ordering in defective perovskite structures is a highly common phenomenon and a family of so-called intergrowth structures can be defined which can be regarded as being composed of structural units of end-member's perovskite and

brownmillerite [15]. Sometimes the structural order and disorder of oxygen vacancies are linked for the same composition by a first-order transition, driven by the gain in the configurational entropy of oxygen vacancies in the disordered structure. Often disordering occurs to a limited degree. Evidence for co-existing populations of ordered and disordered oxygen vacancies in perovskites $La_{0.5}Ba_{0.5}Co_{0.7}Cu_{0.3}O_{3-\delta}$ and $La_{0.6}Sr_{0.4}Co_{0.8}Cu_{0.2}O_{3-\delta}$ and in a number of related compositions was provided by Adler et al. [16] using high temperature ^{17}O NMR. The signal intensity was found to increase steadily with temperature up to the maximum temperature of 950 °C in their experiments, suggesting a concomitant increase in the number of mobile oxygen vacancies. Recent measurements of oxygen permeability and conductivity relaxation on perovskites $La_{1-x}Sr_xCoO_{3-\delta}$ ($x = 0.2$, 0.4 and 0.6) and $La_{0.6}Sr_{0.4}Co_{1-y}Fe_yO_{3-\delta}$ ($x = 0.2$, 0.5 and 0.8) as a function of oxygen partial pressure (10^{-4}–1 bar) and temperature (700–900 °C) made apparent that in these phases the number of mobile oxygen vacancies effectively decreases with lowering p_{O_2} at all temperatures [17,18]. The degree of order is a critical parameter in controlling and optimising the performance of MIEC membranes. Aside from the drop in ionic conductivity at low p_{O_2} values, which limits the oxygen fluxes, the phenomena will induce significant alterations in the chemical potential profile across the ceramic membrane. Opposite from the profile sketched in Fig. 4, steep gradients in μ_{O_2} may appear at the oxygen-lean side of the ceramic membrane. These can produce sufficient local strains in the oxide membrane to cause structural failure.

5. Membrane stability

For syngas production, the MIEC membrane has to operate under severe operating conditions. Performance degradation could occur due to a number of reasons. Besides degradation caused by reaction of the membrane with catalyst or support, or with contaminants, which may be present in both feed gases (e.g. H_2S), decomposition by reduction might occur at the side of the membrane in contact with the syngas. The reduction process progresses into the membrane up to a certain depth, corresponding to the lowest value for the oxygen activity where the oxide is thermodynamically stable (Fig. 5). The membrane will eventually crack due to the volume change accompanying the decomposition.

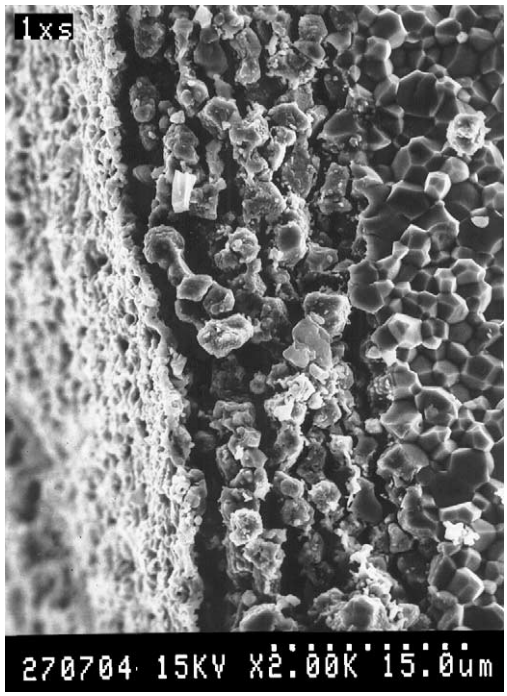

Fig. 5. Cross-sectional SEM image of a $La_{0.6}Sr_{0.4}Fe_{0.8}Fe_{0.2}O_{3-\delta}$ membrane treated for 3 days in 100% CH_4 under permeation conditions at 830 °C. At the immediate surface a porous crust of $SrCO_3$ has formed. Below this layer, basic oxides and possibly elemental Co and Fe are found. At a depth of about 10 μm the perovskite structure is retained.

The stability of undoped perovskites $LaBO_{3-\delta}$, at 1000 °C, is known to decrease in the order $LaCrO_{3-\delta}$ (10^{-20} bar), $LaFeO_{3-\delta}$ (10^{-17} bar), $LaMnO_{3-\delta}$ (10^{-15} bar), $LaCoO_{3-\delta}$ (10^{-7} bar), where the quantity between brackets indicates the oxygen partial pressure below which decomposition of the defective perovskite structure occurs [19] The onset of decomposition shifts to higher oxygen partial pressure upon increased acceptor–dopant concentration (e.g. SrO) [20,21].

Structural failure may occur due to differential stress accompanying the oxygen chemical potential gradient across the MIEC membrane. This is an inevitable concomitant of the expansion of the perovskite unit cell volume with reduction of the transition metal ions to their larger lower-valent forms as the

oxygen partial pressure is lowered. A fracture mechanical analysis of perovskites $La_{0.6}Sr_{0.4}Co_{0.2}Fe_{0.8}O_{3-\delta}$ and the intergrowth phase $SrCo_{0.5}FeO_x$ was recently presented by Hendriksen et al. [22].

Finally, the gradient in the oxygen chemical potential, μ_O, inside a multicomponent oxide $A_{1-x}A'_xBO_{3-\delta}$ induces a corresponding, but inverse gradient of the elemental chemical potentials, as described by the Gibbs–Duhem equation, which reads in differential form:

$$(1-x)\nabla\mu_A + x\nabla\mu_{A'} + \nabla\mu_B + (3-\delta)\nabla\mu_O = 0 \quad (5)$$

If the mobilities of the cations are nonnegligible and different at high temperatures, concentration gradients are developed in such a way that the membrane surface exposed to the higher oxygen partial pressure becomes enriched with the faster moving cation species. Eventually, the multicomponent oxide may decompose even if it is judged to be thermodynamically stable, which is why these processes have been termed kinetic demixing and kinetic decomposition [23,24].

6. Syngas generation

Most active and selective catalysts for the partial oxidation of methane to syngas include Ni-based and noble metal-based catalysts, particularly Rh, supported on ceramic oxides. Since syngas is the thermodynamically favoured product at usual membrane operating temperatures of ~900 °C, yields approach 100% for balanced conditions (i.e. for a 1/2 ratio of O_2/CH_4), and in the presence of a reliable catalyst. The key to success of MIEC membrane-based syngas production rather is to develop a ceramic membrane that combines a high oxygen flux with a long-term mechanical stability in the hostile syngas environment. Table 1 summarises performance values of a number of membrane materials, including the oxygen flux and the reported time on duty.

Though $SrCo_{0.8}Fe_{0.2}O_{3-\delta}$ exhibits a high oxygen flux under air/He conditions [7], Pei et al. [31] found two types of structural failure to occur when membranes were used in syngas generation experiments. Shortly after the reaction started, a failure caused by the lattice expansion mismatch of opposite sides of the membrane occurred. The second type of fracture occurred after days and was the result of chemical decomposition to $SrCO_3$, and elemental Co and Fe. Others have observed membrane failure after a few minutes or hours of operation for membranes fabricated from $La_{0.2}Sr_{0.8}Co_{0.4}Fe_{0.6}O_{3-\delta}$ [25,26] and $La_{0.6}Sr_{0.4}Co_{0.2}Fe_{0.8}O_{3-\delta}$ [32]. In the author's laboratory, membranes made of $La_{0.2}Sr_{0.8}Co_{0.1}Cr_{0.1}Fe_{0.8}O_{3-\delta}$ were used in the conversion of methane to syngas. The membranes cracked after 350 h of operation at 900 °C [28].

Tsai et al. [33] reported that $La_{0.2}Ba_{0.8}Co_{0.2}Fe_{0.8}O_{3-\delta}$ shows higher oxygen fluxes and would be much more stable than $La_{0.2}Sr_{0.8}Co_{0.2}Fe_{0.8}O_{3-\delta}$. The authors successfully used membranes of the latter composition in syngas generation experiments for 850 h at 850 °C, albeit that XRD, EDS and SEM analyses after the experiments revealed morphological and compositional changes of the membrane surfaces. Also noteworthy is that a fivefold increase in the oxygen flux up to a value of 4.3 ml cm^{-2} min was observed by packing the 5% Ni/Al_2O_3 catalyst directly on the membrane reaction-side surface. This observation demonstrates that intimate contact of the catalyst and membrane surface is critical to deplete oxygen at the immediate membrane surface in order to establish a high oxygen potential gradient for oxygen transport. XRD, EDS and SEM analyses however revealed structure and composition changes on the surface.

Table 1
Oxygen flux values observed during syngas generation experiments and reported time on duty

Membrane materials	O_2 flux (ml cm^{-2} min^{-1})	Temperature (°C)	Time on duty (h)	Reference
$SrFeCo_{0.5}O_x$	2–4	850	1000	[25,26]
$Ba_{0.5}Sr_{0.5}Co_{0.8}Fe_{0.2}O_{3-\delta}$	11.5	875	500	[27,44]
$La_{0.8}Sr_{0.2}Co_{0.1}Fe_{0.8}Cr_{0.1}O_{3-\delta}$	14.5	900	340	[28]
$BaCo_{0.4}Fe_{0.4}Zr_{0.2}O_{3-\delta}$	5.6	850	2200	[29]
$La_{0.3}Sr_{1.7}Ga_{0.6}Fe_{1.4}O_{5+\delta}$	6–7	900	1000	[30]

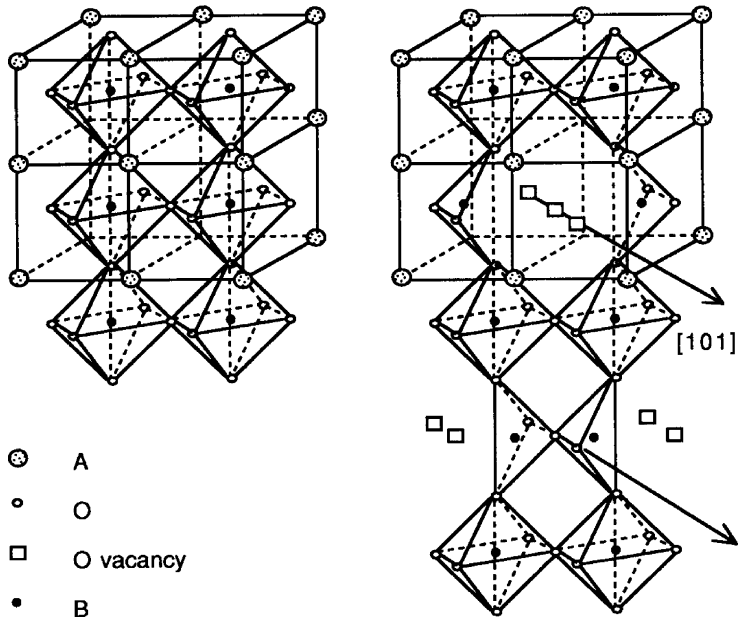

Fig. 6. Idealised structures of (a) cubic perovskite ($CaTiO_3$) and (b) orthorhombic brownmillerite ($Ca_2Fe_2O_5$) lattice with ordered oxygen vacancies along the cubic [1 1 0] direction.

Shao et al. [27,44] successfully operated a reactor for conversion of methane to syngas for more than 500 h using $Ba_{0.5}Sr_{0.5}Co_{0.8}Fe_{0.2}O_{3-\delta}$ as the membrane. At 875 °C, a stable oxygen flux of 11.5 ml cm^{-2} min was observed, the performance being optimised by decreasing the distance between membrane surface and the reforming catalyst. Optimum performance was found in the case when some catalyst particles were deposited on the membrane surface, as revealed by SEM–EDS analysis. Though H_2-TPR experiments demonstrated that the material is not stable under the reducing syngas atmosphere (with a pO_2 of about 10^{-17} bar), the limited kinetics at the reaction-side of the membrane were said to have stabilised the membrane.

An alternative material based on cobalt-doped $Sr_4Fe_6O_{13}$ was developed by Balachandran et al. [2,25,26]. This material adopts an orthorhombic intergrowth structure, consisting of perovskite layers alternating with $Fe_2O_{2.5}$ sesqui-oxide blocks perpendicular to the *b*-axis. Tubular membranes made from $SrCo_{0.5}FeO_x$ ($SrCo_2Fe_4O_{13+\delta}$) could be operated in excess of 1000 h, with oxygen flux values similar to those observed through the cobalt-containing perovskite structures, but yet did not fracture in the process for preparing syngas (Fig. 6). A decline in the oxygen flux (from 4 to 2 ml cm^{-2} min^{-1}) was observed. More recently, it was found that $SrCo_{0.5}FeO_x$ and related compositions $Sr_4(Co_xFe_{1-x})_6O_{13+\delta}$ show multiphase behaviour; the majority phase undergoes decomposition at 900 °C into rock salt and perovskite phases $SrCo_xFe_{1-x}O_{3-\delta}$ at reduced oxygen partial pressures, though the observed phase changes are reversible when the surrounding atmosphere is changed again to air [34]. It is therefore unlikely that compositions based on $SrCo_{0.5}FeO_x$ exhibit long-term stability in syngas generation experiments. Further information about the complex phase behaviour of $SrCo_{0.5}FeO_x$ can be found in a number of papers [35–37]. Xia et al. [38] reported that the oxygen flux for the composition $SrCo_{0.5}FeO_x$ is mainly due to the perovskite phase and not the intergrowth phase.

It is apparent that the cobalt-containing perovskite-related oxides suffer from stability problems in a syngas environment, which might cause membrane failure during long-term operation. This forms a major incentive in several recent studies for either

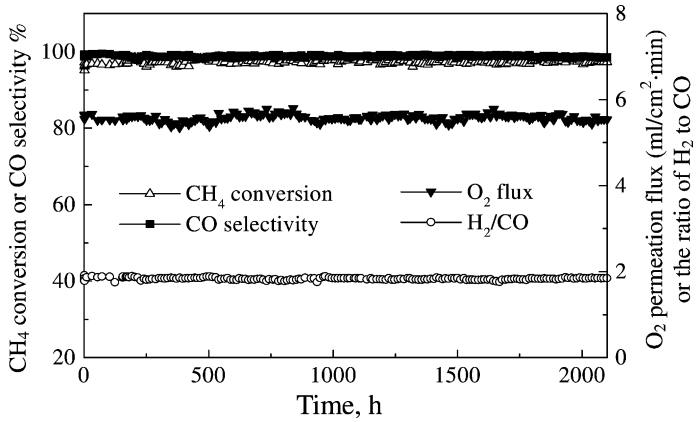

Fig. 7. Long-term stability in CH_4 conversion, CO selectivity, H_2/CO ration and oxygen flux observed in partial oxidation of methane at 850 °C using a $BaCo_{0.4}Fe_{0.4}Zr_{0.2}O_{3-\delta}$ membrane reactor and catalyst LiLaNiO/γ-Al_2O_3 (reprinted from Tong et al. [29]).

lessening the relative amount of cobalt in the perovskite phase, to co-dope the material with less reducible ions, e.g. Zr^{4+}, Ga^{3+} and Al^{3+}, or to add a toughening material such as zirconia or alumina. Tong et al. [29] employed disc membranes fabricated from $BaCo_{0.4}Fe_{0.4}Zr_{0.2}O_{3-\delta}$ in syngas production experiments at 850 °C for more than 2200 h (Fig. 7). XRD, XPS and EDS analyses revealed that slight chemical decomposition had occurred at both membrane surfaces.

Seeking for empirical relationships for predicting oxygen-ionic conductivity in perovskite solid solutions, such as the average metal–oxygen bonding energy, the lattice free volume, and the overall polarisibility, investigators from Eltron Research team have identified mixed-conducting brownmillerite-derived compositions, represented by $La_{2-x}Sr_xGa_{2-y}Fe_yO_{5+\delta}$, reported to be stable over longer periods of time [30]. As mentioned before, the brownmillerite structure must undergo some thermally induced disordering of the oxygen vacancies characteristic for the defective perovskite structure to obtain appreciable levels for the ionic conductivity. The optimised, but classified composition demonstrated continuous performance for over 1 year at a syngas production rate of $60\,ml\,cm^{-2}\,min^{-1}$ (equivalent oxygen flux $10–12\,ml\,cm^{-2}\,min^{-1}$) for the conversion of natural gas into syngas [39]. Eltron Research has teamed with Air Products towards commercialising the membrane technology for CPO of methane to syngas over the next several years.

7. Enhanced selectivity

Obtaining enhanced product selectivity in partial oxidation reactions of hydrocarbons has been another goal of researchers using MIEC membranes. Besides the controlled, distributed supply of oxygen to the side where the catalyst and reactants are located, the oxygen flux may alter the relative presence of different types of active oxygen species (e.g. O^{2-}, O^-, O_2^-) at the membrane surface [40]. These occur as possible intermediates during the recombination of two oxygen anions towards molecular oxygen, which involves a sequence of reaction steps. In a number of studies, the product selectivities in the oxidative coupling of methane are found significantly higher than those obtained in conventional co-feed reactors [41–48]. However, the reported yields are low, generally below 20%, which is mainly attributed to the low intrinsic catalytic activity of the employed MIEC materials in the oxidative coupling reaction, which involves the intermediate formation of methyl radicals $CH_3^{\bullet}$, and to competing reactions in the gas phase. The relatively low oxygen fluxes through current generation of MIEC membranes at intermediate temperatures (∼500 °C) largely limit their use in other partial oxidation reactions.

8. Conclusions and perspectives

The subject of syngas production using MIEC membranes has attracted much interest the past decade

since the economics and environmental benefits are very favourable compared to existing methods. Evaluation indicates that oxygen fluxes are required in the range 5–10 ml cm^{-2} min^{-1} (STP), preferably higher, to achieve the potential benefits [49]. The performance values for selected membrane materials discussed in this review are in this range, while stable continuous operation in a single case has been monitored for over 1 year. Research in coming years will continue in identifying new membrane materials that combine a high oxygen flux with sufficient reliability and durability, and towards developing more efficient routes for membrane fabrication to scale up reactors.

A definite requirement to allow a membrane to function under the severe conditions of syngas production is that it exhibits a high degree of chemical and mechanical stability. Doubts have been expressed of the use of cobalt-containing perovskite membranes, due to their limited stability against reduction. Partial decomposition of the membrane surface up to certain depth as a result of exposure to the reducing syngas environment must certainly be avoided, if it were to be tolerated at all, to avert the risk of mechanical failure. A challenge facing researchers in this area is therefore to understand the critical roles reactor design, reaction kinetics and addition of possible substituents to the methane feed stream (e.g. H_2O) play in determining the oxygen activity at the immediate membrane surface so as to avoid reduction of the membrane material.

A major barrier to technological application is the high operating temperature to obtain acceptable oxygen fluxes. Many technical hurdles need to be overcome. Besides issues related to membrane stability and integrity with respect to other reactor components, one of the key problems is the development of seals for the ceramic elements that are able to operate at these high temperatures. In addition to syngas production, many other market opportunities exist if the temperature of membrane operation could be lowered without sacrificing the oxygen fluxes. The development of such membranes operating at moderate temperatures poses a key challenge to material scientists in this area. The use of supported thin-film membranes will definitely allow a substantial reduction in operating temperature as was demonstrated in recent studies [50,51]. Additionally, we need an improved understanding of the role of extended defect interactions, and onset of locally ordered arrangements of oxygen vacancies, in determining the oxygen fluxes, and how these can be manipulated when optimised performance is to be achieved. Most of the present research is focused on syngas production. Existing literature data clearly demonstrates the principal feasibility of the concept. The ability for using MIEC membranes in reactors for the oxidative dehydrogenation of ethane or propane, or for the direct conversion of methane to methanol or formaldehyde is tantalising, and yet represents another challenge.

References

[1] H.J.M. Bouwmeester, A.J. Burggraaf, in: P.J. Gellings, H.J.M. Bouwmeester (Eds.), CRC Handbook of Solid State Electrochemistry, CRC Press, Boca Raton, FL, 1997, Chapter 14.
[2] U. Balachandran, J.T. Dusek, S.M. Sweeney, R.B. Poebbel, R.L. Mieville, P.S. Mayia, M.S. Kleefish, S. Pei, T.P. Kobylinski, C.A. Udovich, A. Bose, Am. Ceram. Soc. Bull. 74 (1995) 71.
[3] C.Y. Tsai, A.G. Dixon, W.R. Moser, Y.H. Ma, AIChE J. 43 (1997) 2741.
[4] C. Tsai, A.G. Dixon, Y.H. Ma, W.R. Moser, M. Pascucci, J. Am. Ceram. Soc. 81 (1998) 1437.
[5] T. Ishihara, Y. Takita, Catal. Surv. Jpn. 4 (2000) 125.
[6] P.N. Dyer, R.E. Richards, S.L. Russek, D.M. Taylor, Solid Sate Ionics 134 (2000) 21.
[7] Y. Teraoka, H.M. Zhang, S. Furukawa, N. Yamazoe, Chem. Lett. (1985) 1743.
[8] Y. Teraoka, T. Nobunaga, N. Yamazoe, Chem. Lett. (1988) 503.
[9] Y. Teraoka, H.M. Zhang, K. Okamoto, N. Yamazoe, Mater. Res. Bull. 23 (1988) 51.
[10] C. Wagner, W. Schottky, Z. Phys. Chem. B 11 (1930) 25.
[11] J. Mizusaki, M. Yoshihiro, S. Yamauchi, K. Fueki, J. Solid State Chem. 58 (1985) 257.
[12] J.E. ten Elshof, H.J.M. Bouwmeester, H. Verweij, Solid State Ionics 81 (1995) 97.
[13] T. Kudo, in: P.J. Gellings, H.J.M. Bouwmeester (Eds.), CRC Handbook of Solid State Electrochemistry, CRC Press, Boca Raton, FL, 1997, Chapter 6.
[14] D.M. Smyth, Ann. Rev. Mater. Sci. 15 (1985) 329–357.
[15] D.M. Smyth, Cryst. Latt. Def. Amorph. Mater. 18 (1989) 355–375.
[16] S. Adler, S. Russek, J. Reimer, N. Fendorf, A. Stacy, Q. Huang, A. Santoro, J. Lynn, J. Baltisberger, U. Werner, Solid State Ionics 68 (1994) 193–211.
[17] L.M. van der Haar, M.W. den Otter, M. Morskate, H.J.M. Bouwmeester, H. Verweij, J. Electrochem. Soc. 149 (2002) J41.
[18] M.W. den Otter, Ph.D. Thesis, University of Twente, The Netherlands, 2000.
[19] T. Nakamura, G. Petzow, L.J. Gauckler, Mater. Res. Bull. 14 (1979) 649.

[20] B.C.H. Steele, Mater. Sci. Eng. B 13 (1992) 79.
[21] H.U. Anderson, Solid State Ionics 52 (1992) 33–41.
[22] P.V. Hendriksen, P.H. Larsen, M. Mogensen, F.W. Poulsen, K. Wiik, Catal. Today 56 (2000) 283.
[23] H. Schmalzried, W. Laqua, P.L. Lin, Z. Naturforsch. A 34 (1979) 192–199.
[24] H. Schmalzried, W. Laqua, Oxid. Met. 15 (1981) 339–353.
[25] U. Balachandran, J.T. Dusek, R.L. Mieville, R.B. Poeppel, M.S. Kleefisch, S. Pei, T.P. Kobylinski, C.A. Udovich, A.C. Bose, Appl. Catal. A 133 (1995) 19–29.
[26] U. Balachandran, J.T. Dusek, P.S. Maiya, B. Ma, R.L. Mieville, M.S. Kleefisch, C.A. Udovich, Catal. Today 36 (1997) 265.
[27] Z. Shao, G. Xiong, H. Dong, W. Yang, L. Lin, Sep. Purif. Technol. 25 (2001) 97–116.
[28] B. McCool, University of Twente, The Netherlands, Unpublished results, 2000.
[29] J. Tong, W. Yang, R.C. Baichun Zai, L. Lin, Catal. Lett. 78 (2002) 129.
[30] M. Schwartz, J.H. White, A.F. Sammels, US Patent 6 033 632 (2000).
[31] S. Pei, M.S. Kleefish, T.P. Kobylinski, J. Faber, C.A. Udovich, V. Zhang-McCoy, B. Dabrowski, U. Balachandran, R.L. Mieville, R.B. Poeppel, Catal. Lett. 30 (1995) 201.
[32] W.Q. Jin, S.G. Li, P. Huang, N.P. Xu, J. Shi, Y.S. Lin, J. Membr. Sci. 166 (2000) 13.
[33] C.Y. Tsai, A.G. Dixon, W.R. Moser, Y.H. Ma, AIChE J. 43 (1997) 2741.
[34] B.J. Mitchell, J.W. Richardson, C.D. Murphy, B. Ma, U. Balachandran, J.P. Hodges, J.D. Jorgensen, Mater. Res. Bull. 35 (2000) 491.
[35] S. Guggilla, A. Mantahiram, J. Electrochem. Soc. 144 (1997) L120.
[36] H. Fjellvag, B.C. Hauback, R. Bredesen, J. Mater. Chem. 7 (1997) 2415.
[37] S. Kim, Y.L. Yang, R. Christoffersen, A.J. Jacobson, Solid State Ionics 109 (1998) 187.
[38] Y. Xia, T. Armstrong, F. Prado, A. Mantahiram, Solid State Ionics 130 (2000) 81.
[39] A.F. Sammells, M. Schwartz, R.A. Mackay, T.F. Barton, D.R. Peterson, Catal. Today 56 (2000) 325.
[40] P.J. Gellings, H.J.M. Bouwmeester, Catal. Today 12 (1992) 1.
[41] J.E. ten Elshof, H.J.M. Bouwmeester, H. Verweij, Appl. Catal. A 130 (1995) 195.
[42] J.E. ten Elshof, B.A. van Hassel, H.J.M. Bouwmeester, Catal. Today 25 (1995) 397.
[43] S. Xu, W. Thomson, AIChE J. 43 (1997) 2731.
[44] Z. Shao, H. Dong, G. Xiong, Y. Cong, W. Yang, J. Membr. Sci. 183 (2001) 181.
[45] Y.S. Lin, Y. Zeng, J. Catal. 164 (1996) 220.
[46] Y. Zeng, Y.S. Lin, Ind. Eng. Chem. Res. 36 (1997) 277.
[47] Y. Lu, A.G. Dixon, W.R. Moser, Y.H. Ma, U. Balachandran, Catal. Today 56 (2000) 297.
[48] Y. Lu, A.G. Dixon, W.R. Moser, Y.H. Ma, U. Balachandran, J. Membr. Sci. 170 (2000) 27.
[49] R. Bredesen, J. Sogge, A technical and economic assessment of membrane reactors for hydrogen and syngas production, SINTEF report S96017, 1996.
[50] J.T. Ritchie, J.T. Richardson, D. Luss, AIChE J. 47 (2001) 2092.
[51] L.M. van der Haar, Ph.D. Thesis, University of Twente, The Netherlands, 2001.